Research Article

Received: 14 May 2012 Revised: 14 August 2012 Accepted: 2 October 2012 Published online in Wiley Online Library: 4 December 2012

(wileyonlinelibrary.com) DOI 10.1002/jctb.3977

Electrochemical synthesis of cuprous oxide with a cylindrical bipolar reactor

Omar González Pérez and José M. Bisang*

Abstract

BACKGROUND: This work analyzes the behaviour of monopolar and bipolar electrochemical reactors with a cylindrical configuration using woven wire meshes as three-dimensional anodes for the production of cuprous oxide.

RESULTS: Calcium gluconate as an additive diminishes cell voltage because of the depolarization of the hydrogen evolution reaction, and it also avoids the reduction of cuprous oxide to metallic copper. The quality of the powders obtained in a bipolar reactor with three-dimensional anodes is similar to that of a monopolar reactor. Powders containing 97% cuprous oxide were obtained at current densities ranging from 21 to 103 mA cm^{-2} with current efficiencies near 100%. The bipolar arrangement presents a simpler electrical connection; however, special attention must be paid to some features of construction to minimize the leakage current.

CONCLUSION: Cylindrical bipolar electrochemical reactors with three-dimensional anodes show a good performance for the production of cuprous oxide powder.

Keywords: cuprous oxide; electrochemical reactor; bipolar electrode; three-dimensional electrode

NOTATION

CSA	cross-sectional area of the interelectrode gap (cm^2)
d	electrode diameter (mm)
E_{SCE}	electrode potential referred to saturated calomel electrode (V)
I	current (A)
j	current density (mA cm^{-2})
L	length of the woven wire mesh (cm)
S	projected internal electrode surface area (cm^2)
t	time of the experiment (min)
T	temperature (°C)
U	cell voltage (V)
β	anodic current efficiency for cuprous oxide production (%)
γ	current efficiency for hydrogen evolution (%)
Δr_{mesh}	thickness of the mesh packing (mm)
Δr_{wall}	thickness of the copper tube (mm)

Subscripts

A	terminal anode
B	bipolar electrode
C	terminal cathode
ext	external
int	internal
mean	mean value
SCE	saturated calomel electrode

INTRODUCTION

Cuprous oxide (Cu_2O) is used in many different ways: as a reducing agent in agricultural chemicals, as a pigment for ceramics and to prepare marine antifouling paints, as a precursor for a range of copper chemicals and as a material for solar cells.[1,2] Cuprous oxide powder can be produced by pyrometallurgical methods,[3,4] which require a rigorous control of temperature to avoid the production of mixtures of the two copper oxides together or with metallic copper. Likewise, various hydrometallurgical processes can be used to prepare cuprous oxide,[3] which can also be produced by the reduction of copper(II) salts or cupric oxide under alkaline conditions.[5,6] Depending on the reducing agent used and its strength, the reduction rate may be slow and the final product impure, whereas the amount of the reagent must be adequately controlled to avoid metallic copper formation. Alternatively, cuprous oxide can be produced by hydrolysis from a two-phase aqueous–organic system.[7] The electrolytic procedure can overcome the shortcomings of the other methods and is recognized as an appropriate and versatile means of producing cuprous oxide. Vetere and Romagnoli[8–10] proposed as electrolyte an alkaline solution of sodium chloride and sodium nitrate. Hydroxylamine is formed at the cathode, which precludes hydrogen evolution and reduces the cupric compounds to cuprous species. Thus, an electrochemical reactor without a separator was used to produce cuprous oxide of high purity. The basic electrode reactions were studied[11] taking into account the concentration of sodium chloride, alkalinity, temperature, additives, current density

* *Correspondence to: José M. Bisang, Programa de Electroquímica Aplicada e Ingeniería Electroquímica (PRELINE), Facultad de Ingeniería Química, Universidad Nacional del Litoral, Santiago del Estero 2829, S3000AOM Santa Fe, Argentina. Email: jbisang@fiq.unl.edu.ar*

Programa de Electroquímica Aplicada e Ingeniería Electroquímica (PRELINE), Facultad de Ingeniería Química, Universidad Nacional del Litoral, Santiago del Estero 2829, S3000AOM, Santa Fe, Argentina

and the effect of carbonate ions. Likewise, the operating conditions were also tested on a laboratory-scale reactor[12] and powders with 95% of purity with a colour suitable for use in antifouling paints were produced in a pilot plant cell.[13] The electrosynthesis of cuprous oxide was examined using a titanium mesh basket loaded with small pieces of high-grade copper scrap as an anode.[14] Moreover, the simultaneous production of cuprous oxide at the anode and metallic nickel at the cathode was analyzed in a two-compartment reactor.[15] In general, it is accepted that an aqueous solution of sodium chloride, 250 g dm^{-3} at pH 10 and 80°C, represents suitable conditions for the production of cuprous oxide. However, the optimal current density is controversial, depending on the type of the reactor and additives employed.

In previous studies, the electrodes were arranged in a monopolar configuration requiring an external electrical connection at each electrode of the reactor, which can be troublesome. The bipolar arrangement is interesting because the connection is reduced only to the terminal electrodes and each intermediate electrode works on one side as a cathode and on the opposite side as an anode. Electrochemical reactors with bipolar parallel plate electrodes are common in industrial practice and the state of the art is properly shown by Pletcher and Walsh.[16] However, the main drawback of this configuration is the presence of a leakage current, which bypasses the bipolar electrodes flowing through the solution phase outside the interelectrode gap without producing electrochemical reactions. Then, an appropriate design of the electrochemical reactor is required to minimize this negative aspect.

The aim of the present contribution was to corroborate the best electrical conditions for the production of cuprous oxide using a rotating disc electrode, which represents a system with well-defined hydrodynamic conditions, and to check the performance of a cylindrical bipolar electrochemical reactor on a laboratory scale. Likewise, three-dimensional structures were examined as an anode with the purpose of using scrap copper for the production of cuprous oxide.

FUNDAMENTAL STUDIES WITH ROTATING DISC ELECTRODES

Experimental details

A rotating disc electrode was used to obtain anodic and cathodic polarization curves. The working electrode was a copper disc, 3 mm in diameter embedded in a 10 mm diameter Teflon cylinder. A platinum wire, 1 mm diameter and 100 mm long, was used as a counter electrode. A saturated calomel electrode was used as reference and the potentials are referred to this electrode.

The surface of the working electrode was polished to a bright mirror finish with a slurry of 0.3 μm alumina powder and it was copiously washed with distilled water. According to previous studies,[11,12] the electrolyte was 250 g dm^{-3} NaCl at pH 10 with the addition of NaOH. In some experiments calcium gluconate, 5 g dm^{-3}, was added to analyze its influence on the copper oxide reduction. All experiments were performed at 80°C, 1000 rpm rotation speed and under a slow potentiodynamic sweep of 1 mV s^{-1} in order to obtain steady-state polarization curves. Nitrogen was bubbled into the reactor prior to the experiment to remove the dissolved oxygen.

Results and discussion

Figure 1 shows anodic polarization curves for the supporting electrolyte and also with the addition of calcium gluconate and cuprous oxide. The following reactions occurred at the anode-electrolyte bulk:

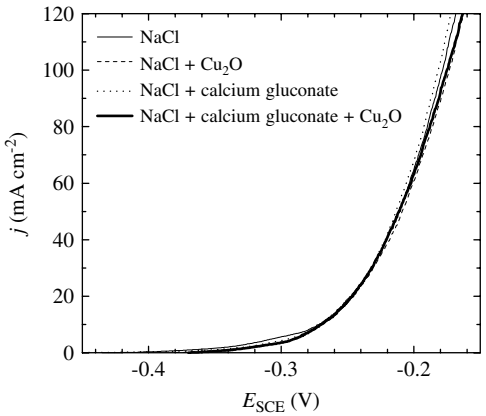

Figure 1. Anodic current density as a function of the electrode potential for the supporting electrolyte and with the addition of calcium gluconate and cuprous oxide. $T = 80^{\circ}C$. Rotation speed: 1000 rpm. Potential sweep rate: 1 mV s^{-1}.

$$2\,Cu + 2\,OH^- \rightarrow Cu_2O + H_2O + 2\,e^-$$
$$E_{0,SCE}\left(80^{\circ}C, pH\ 10\right) = -0.4665\ V \quad (1)$$

and

$$Cu + 2\,OH^- \rightarrow CuO + H_2O + 2\,e^-$$
$$E_{0,SCE}\left(80^{\circ}C, pH\ 10\right) = -0.3604\ V \quad (2)$$

Combining Equations (1) and (2) the anodic processes can be represented by:

$$(1+\beta)\ Cu + 2\,OH^- \rightarrow \beta Cu_2O + (1-\beta)\ CuO + H_2O + 2\,e^- \quad (3)$$

where β is the anodic current efficiency for cuprous oxide production. Thus, when β approaches unity, reaction (1) occurs and when β equals zero cupric oxide is produced. The dissolution of copper to form cuprous oxide is thermodynamically favoured. However, the difference between the equilibrium potentials of reactions (1) and (2) is only 0.106 V, which suggests a careful control of anodic potential to prevent the formation of cupric oxide. Figure 1 shows that copper dissolution begins near −0.450 V, which is approximately in accordance with the equilibrium potential predicted by the Nernst equation for cuprous oxide formation, reaction (1). However, a substantial current is only observed at more anodic potentials and the polarization curves are similar for all the electrolytes. Then, the addition of calcium gluconate or the presence of cuprous oxide has no influence on copper dissolution. Moreover, a potential to separate both anodic reactions cannot be identified from the polarization curves.

The cathodic polarization curves for the supporting electrolyte and also with the addition of calcium gluconate and cuprous oxide are reported in Fig. 2. At the cathode, the competitive reactions occurred:

$$\left(2\,H_2O + 2\,e^- \rightarrow H_2 + 2\,OH^-\right)\gamma \quad (4)$$

and

$$\left(Cu_2O + H_2O + 2\,e^- \rightarrow 2\,Cu + 2\,OH^-\right)\ (1-\gamma) \quad (5)$$

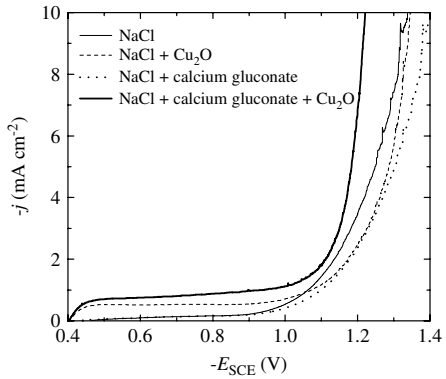

Figure 2. Cathodic current density as a function of the electrode potential for the supporting electrolyte and with the addition of calcium gluconate and cuprous oxide. $T = 80^{\circ}C$. Rotation speed: 1000 rpm. Potential sweep rate: 1 mV s^{-1}.

where γ is the current efficiency for hydrogen evolution. Combining Equations (4) and (5) the cathodic processes are represented by:

$$(1+\gamma)\ H_2O + (1-\gamma)\ Cu_2O + 2\,e^- \rightarrow 2\,(1-\gamma)\ Cu + \gamma H_2 + 2\,OH^- \quad (6)$$

Considering Equations (3) and (6), the overall reaction in the electrochemical reactor is given by:

$$(\beta + 2\gamma - 1)\ Cu + \gamma H_2O \rightarrow (\beta + \gamma - 1)\ Cu_2O + (1-\beta)\ CuO + \gamma H_2 \quad (7)$$

When $\beta = \gamma = 1$ Equation (7) is simplified to:

$$2\,Cu + H_2O \rightarrow Cu_2O + H_2 \quad (8)$$

which represents a more efficient behaviour for the electrochemical reactor. Then, as expected, all efforts must be oriented to increase current efficiencies at both electrodes.

Figure 2 shows that for the supporting electrolyte and also with calcium gluconate as additive, the main cathodic reaction is the hydrogen evolution. However, a limiting current density is observed when cuprous oxide is dispersed in the electrolyte, assigned to its reduction to metallic copper, which occurs before hydrogen evolution takes place. Then, to minimize the detrimental effect of reaction (5) on the performance of an electrochemical reactor for cuprous oxide production, it is convenient that the surface area of the cathode be smaller than that of the anode. Thus, the current at the cathode is preferentially undertaken by hydrogen evolution and the reconversion of cuprous oxide to metallic copper is diminished. In the case of a cylindrical arrangement the cathode must be the central electrode. Furthermore, the simultaneous addition of cuprous oxide and calcium gluconate shifts the hydrogen evolution reaction to more positive potentials thereby, lowering cell voltage, which can be recognized as the first beneficial aspect of calcium gluconate as an additive for cuprous oxide production.[11]

EXPERIMENTS WITH CYLINDRICAL BATCH REACTORS

Experimental details

The experiments were performed in two batch reactors (70 mm internal diameter × 90 mm high and 100 mm internal diameter × 105 mm high) with cylindrical concentric electrodes. The reactors were thermostated at 80°C by a heating jacket. The terminal anode and the bipolar electrodes were made by setting a cylindrical stack of copper woven wire meshes (50-mesh size, 0.22 mm wire diameter and 0.28 mm distance between wires) on the inner surface of a copper tube. This tube works as an anodic current feeder for the terminal anode and as a partition wall for the bipolar electrodes in order to minimize the leakage current. Likewise, the outer surface of the partition wall is the cathodic side of the bipolar electrode, whereas its anodic side is the packing of the copper woven wire meshes. Following this procedure five three-dimensional electrodes were constructed, summarized in Table 1, which can be alternatively arranged as a terminal anode or as a bipolar electrode. Two copper bars (Cathode 1: 6.15 mm diameter, 13.52 cm^2 surface area; Cathode 2: 11.75 mm diameter, 25.84 cm^2 surface area, both 70 mm high) were alternatively used as a terminal cathode. The combination of the five three-dimensional electrodes with the two terminal cathodes enabled different reactor configurations either under monopolar connection or with one bipolar electrode, which is sketched in Fig. 3. All the experiments were performed under galvanostatic control.

Table 1. Dimensions of the three-dimensional electrodes

	Electrode 1	Electrode 2	Electrode 3	Electrode 4	Electrode 5
d_{ext} (mm)	98.53	63.88	51.04	36.00	31.68
Δr_{wall} (mm)	1.38	1.85	1.29	1.30	1.50
d_{int} (mm)	91.95	54.42	44.02	27.64	25.78
Δr_{mesh} (mm)	1.91	2.88	2.22	2.88	1.45
L (cm)	100.00	100.00	60.00	56.10	26.00
S (cm^2)	202.21	119.68	96.81	60.78	56.69

After each run, the terminal anode and the bipolar electrode were washed with distilled water to pick up the cuprous oxide powder retained inside the three-dimensional structure. Then, the electrodes were treated with hydrochloric acid to remove the remaining cuprous oxide and they were washed with distilled water. The loss of weight was measured after drying off these electrodes in a vacuum oven at 45°C. The current efficiency for the anodic cuprous oxide formation, β, at each electrode was calculated applying the Faraday law.

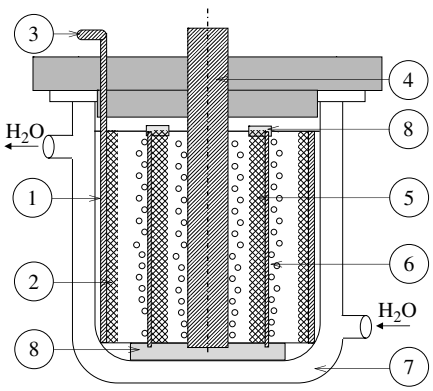

Figure 3. Schematic view of a batch electrochemical reactor with one bipolar three-dimensional electrode. 1, terminal anode; 2, copper woven wire meshes; 3, anodic current feeder; 4, terminal cathode; 5, anodic side of the bipolar electrode; 6, cathodic side of the bipolar electrode; 7, heating jacket; 8, plastic protectors.

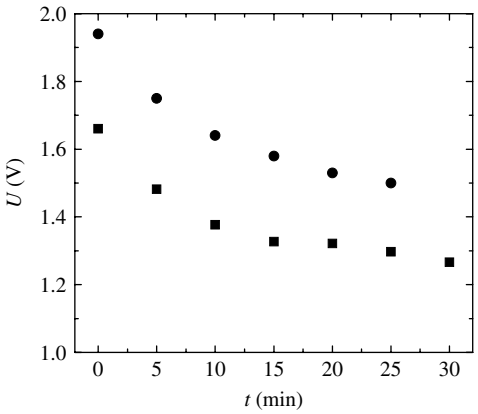

Figure 4. Cell voltage as a function of time. Monopolar connection. Anode: Electrode 2; cathode: Cathode 2. $I = 3$ A, $j_A = 25.07$ mA cm^{-2}, $j_C = 116.10$ mA cm^{-2}. Electrolyte: 250 g dm^{-3} NaCl, pH = 10, $T = 80^\circ$C. ● without calcium gluconate; ■ with calcium gluconate, 5 g dm^{-3}.

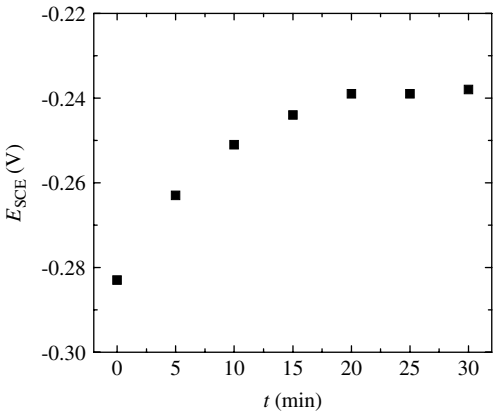

Figure 5. Anode potencial as a function of time. Monopolar connection. Anode: Electrode 2; cathode: Cathode 2. $I = 3$ A, $j_A = 25.07$ mA cm^{-2}, $j_C = 116.10$ mA cm^{-2}. Electrolyte: 250 g dm^{-3} NaCl, 5 g dm^{-3} calcium gluconate, pH = 10, $T = 80^\circ$C.

Furthermore, copper particles were observed in the powders produced with a three-dimensional anode, which can be attributed to its mechanical deterioration. Then, the powders were treated by fractional sedimentation in a decanter to separate two fractions. The upper one, approximately 70% of the total powder and free of copper particles, was used to determine the powder composition. This fraction was profusely washed with distilled water and with a solution of invert sugar at 3%, centrifuged and dried in a vacuum oven at 45°C. Its metallic copper concentration was determined by the procedure reported by Vetere and Romagnoli[9] and the total reducing power was analyzed according to the ASTM Specification D912-81. Then, the cuprous oxide concentration was obtained as the difference between the total reducing power and the metallic copper concentration. The cupric oxide content was calculated as the difference between the mass of the sample and the total reducing power. Some powders were examined by scanning electron microscopy (SEM) to determine their morphologies.

Results and discussion

Figure 4 compares the cell voltage for two experiments under monopolar connection, with and without the addition of calcium gluconate. As expected, the presence of calcium gluconate diminishes the cell voltage by approximately 0.2 V because of the depolarization of the hydrogen evolution reaction.[11] In the experiment without calcium gluconate, the formation of a spongy precipitate of copper around the cathode was observed as a consequence of reaction (5) and also due to the reduction of cuprous oxide by the hydrogen evolved at the cathode.[9] Hence, the copper composition of the powder was 15.1% for the experiment without calcium gluconate and 0.4% when this additive was used. Therefore, the inhibition of cuprous oxide reduction to metallic copper can be recognized as a second beneficial aspect of the calcium gluconate addition. Comparing this conclusion with the polarization curves reported in Fig. 2, where no inhibition was detected when the cuprous oxide reduction takes place as a sole reaction at the cathode, it has to be accepted that the inhibiting effect of the calcium gluconate on the cuprous oxide reduction is only successful at very negative cathodic potentials, at which hydrogen evolution simultaneously takes place. This effect may be explained by its adsorption on the copper cathode hindering the reduction of the cuprous oxide particles.[17]

The anode potential of the above monopolar experiment with calcium gluconate is reported in Fig. 5, where it is observed that the potential approaches −0.24 V for 25.07 mA cm^{-2} of anodic current density referred to the internal projected area of the three-dimensional electrode, 119.68 cm^2. This current density is in close agreement with the value measured with the rotating disc electrode and reported in Fig. 1, despite the geometric and hydrodynamic differences between the two reactors, which corroborates a charge transfer kinetic control for copper dissolution in the potential range examined.

Table 2 reports the geometric dimensions of the reactor arrangements used in this contribution and Table 3 summarizes the experimental conditions. The first three rows in both tables correspond to experiments with a monopolar connection, where the anodic current efficiency higher than 100% can be attributed to the loss of weight due to mechanical deterioration of the electrode because of the uneven dissolution of the copper mesh. The experiment reported in the fourth row in Table 3 shows a low value of current efficiency at the bipolar electrode. In the experiment included in the fifth row, plastic woven mesh separators were placed both around the terminal cathode and at the cathodic side of the bipolar electrode to avoid the hydrogen oxidation reaction at the anodes. However, no significant increase in the anodic current efficiency at the bipolar electrode was observed. Then, hydrogen oxidation can be disregarded as an anodic reaction. The experiments reported between the sixth and ninth rows in Table 3 were performed changing the operating conditions and the geometrical parameters. The current efficiency as a function of the interelectrode gap is given in Fig. 6 and as a function of the cross-sectional area of the interelectrode gap in Fig. 7. It can be observed that the current efficiency at the terminal anode is always higher than 100% independent of the geometrical dimensions of the interelectrode gap, which shows that the interelectrode gap has no influence on the reactor performance. However, the current efficiency at the bipolar anode is always lower than 100%. The scattering of the results for similar values of the interelectrode gap is due to the fact that the experiments were performed at different currents. Nevertheless, the anodic current efficiency at the bipolar electrode shows a tendency to decrease when the cell voltage increases as shown in Fig. 8, which can be attributed either to the leakage current by-passing the bipolar electrode or to the formation of cupric oxide as an alternative anodic reaction. In order

Table 2. Dimensions of the different reactor arrangements

Reactor	Terminal anode	Bipolar electrode	Terminal cathode	Interelectrode gap (mm)	*CSA* (cm^2)
1	Electrode 2	—	Cathode 2	Gap = 21.34	22.18
2	Electrode 1	—	Cathode 1	Gap = 42.90	66.11
3	Electrode 3	—	Cathode 2	Gap = 16.14	14.13
4	Electrode 2	Electrode 4	Cathode 2	$Gap_{A-B} = 9.21$	$CSA_{A-B} = 13.08$
				$Gap_{B-C} = 7.95$	$CSA_{B-C} = 4.92$
5	Electrode 1	Electrode 3	Cathode 1	$Gap_{A-B} = 20.46$	$CSA_{A-B} = 45.94$
				$Gap_{B-C} = 18.94$	$CSA_{B-C} = 14.92$
6	Electrode 1	Electrode 5	Cathode 2	$Gap_{A-B} = 30.14$	$CSA_{A-B} = 58.52$
				$Gap_{B-C} = 7.02$	$CSA_{B-C} = 4.14$
7	Electrode 1	Electrode 2	Cathode 1	$Gap_{A-B} = 14.04$	$CSA_{A-B} = 34.35$
				$Gap_{B-C} = 24.14$	$CSA_{B-C} = 22.96$

Table 3. Summary of experimental conditions

Reactor (Experiment)	*I* (A)	*t* (min)	U_{mean} (V)	j_A (mA cm^{-2})	j_C (mA cm^{-2})	j_B (mA cm^{-2})	β_A (%)	β_B (%)
1[a]	3.0	30	1.390	25.07	116.10	—	96.44	—
2[a]	5.0	30	2.047	24.73	369.82	—	104.09	—
3[a]	2.5	36	1.339	25.82	96.75	—	108.53	—
4	4.0	22.5	2.602	33.42	154.80	65.81	112.19	50.74
4[b]	3.0	30	2.777	25.07	116.10	49.36	108.81	52.35
5 (1)	2.11	60	2.277	10.43	156.07	21.80	106.42	71.22
5 (2)	4.67	19.27	2.955	23.09	345.41	48.24	108.84	27.36
6	1.5	60	2.175	7.42	58.05	26.46	112.75	41.32
7	3.0	30	2.337	14.84	221.89	25.07	109.38	64.67
5[c](1)	2.0	63.25	2.354	9.89	147.93	20.66	118.43	94.02
5[c](2)	2.5	50.6	2.404	12.36	184.91	25.82	109.02	98.22
5[c](3)	3.0	42.17	2.576	14.84	221.89	30.99	111.22	100.82
5[c](4)	4.2	30.12	2.773	20.77	310.65	43.38	106.02	98.02
5[c](5)	6.0	21.08	3.185	29.67	443.79	61.98	111.02	106.02
5[c](6)	10.0	12.65	3.826	49.45	739.64	103.30	109.42	104.22
5[c](7)	19.0	6.66	5.554	93.96	1405.33	196.26	118.83	111.42

[a] Monopolar.
[b] Cathodic side of the bipolar electrode and terminal cathode with a woven plastic separator.
[c] Plastic protectors in the upper and lower parts of the bipolar electrode.

to circumvent these disjunctive propositions, in the experiments reported in the last rows of Table 3 performed with the reactor 5[c], the lower ends of the electrodes were inserted in a plastic disc and the upper end of the bipolar electrode was covered with a Teflon disc in order to prevent the leakage currents. An increase in the anodic current efficiency at the bipolar electrode was observed with this modification. The low values of anodic current efficiencies at the bipolar electrodes in the experiments shown from rows 4 to 9 can be mainly attributed to the leakage current, which confirms that the use of bipolar electrodes requires special attention in the reactor design to minimize the leakage current.

Table 4 summarizes the concentrations of powders in typical experiments. As a comparison, the first row shows the powder composition obtained in an experiment with monopolar connection. The second row corresponds to the experiment with a plastic woven mesh around the terminal cathode and also at the cathodic side of the bipolar electrode, which restricts the contact between the cuprous oxide formed near the anode with the hydrogen evolved at the cathode; hydrogen may be a reducing agent for the cuprous compound.[9] The experiment listed in the third row was done without a separator. It can be observed

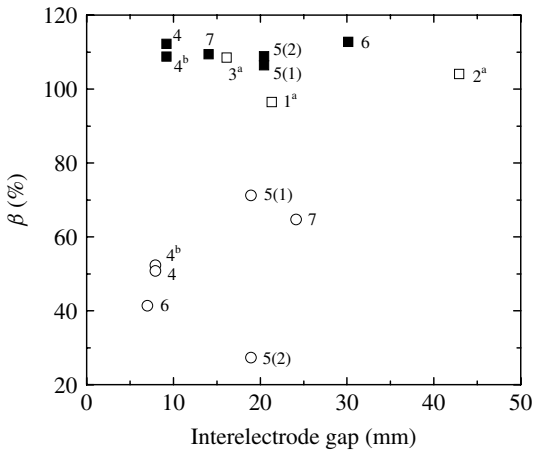

Figure 6. Anodic current efficiency for the terminal anode and for the bipolar electrode as a function of the interelectrode gap. □ Monopolar anode, ■ Terminal anode, ○ Bipolar electrode. Electrolyte: 250 g dm^{-3} NaCl, 5 g dm^{-3} calcium gluconate, pH = 10, $T = 80^{\circ}C$. Reference at each experimental point according to the first column of Table 3.

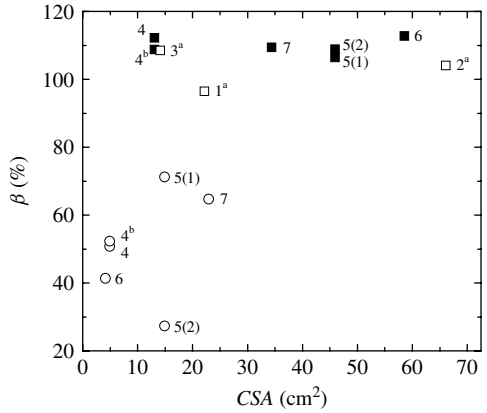

Figure 7. Anodic current efficiency for the terminal anode and for the bipolar electrode as a function of the cross-sectional area of the interelectrode gap. □ Monopolar anode, ■ Terminal anode, ○ Bipolar electrode. Electrolyte: 250 g dm^{-3} NaCl, 5 g dm^{-3} calcium gluconate, pH = 10, $T = 80^{\circ}C$. Reference at each experimental point according to the first column of Table 3.

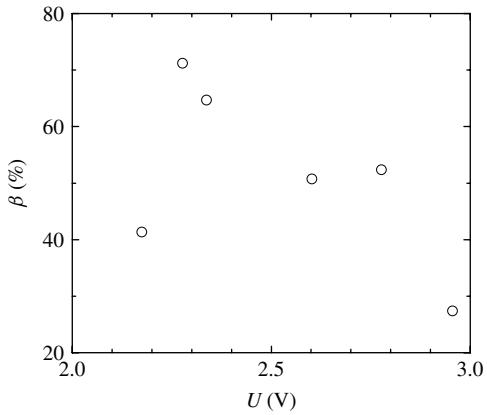

Figure 8. Anodic current efficiency at the bipolar electrode as a function of the cell voltage. Reactors 4, 4^b, 5, 6 and 7. Electrolyte: 250 g dm^{-3} NaCl, 5 g dm^{-3} calcium gluconate, pH = 10, $T = 80^{\circ}C$.

Table 4. Summary of the quality of cuprous oxide powders

Reactor (Experiment)	wt% Cu_2O	wt% Cu	wt% CuO
1[a]	93.22	0.40	6.37
4[b]	93.30	0.00	6.70
4	93.46	0.72	5.83
5[c](1)	80.61	5.36	14.03
5[c](2)	89.82	1.32	8.86
5[c](3)	82.44	6.38	11.18
5[c](4)	97.21	0.48	2.31
5[c](5)	96.60	0.00	3.40
5[c](6)	97.38	1.12	1.50
5[c](7)	93.30	1.00	5.70

[a] Monopolar.
[b] Cathodic side of the bipolar electrode and terminal cathode with a woven plastic separator.
[c] Plastic protectors in the upper and lower parts of the bipolar electrode.

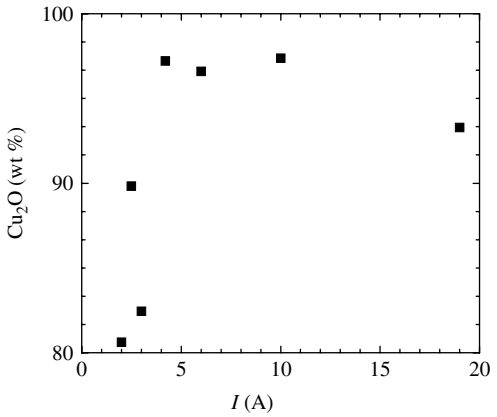

Figure 9. Cuprous oxide concentration in the powder as a function of the total cell current. Reactor 5^c. Electrolyte: 250 g dm^{-3} NaCl, 5 g dm^{-3} calcium gluconate, pH = 10, $T = 80^{\circ}C$.

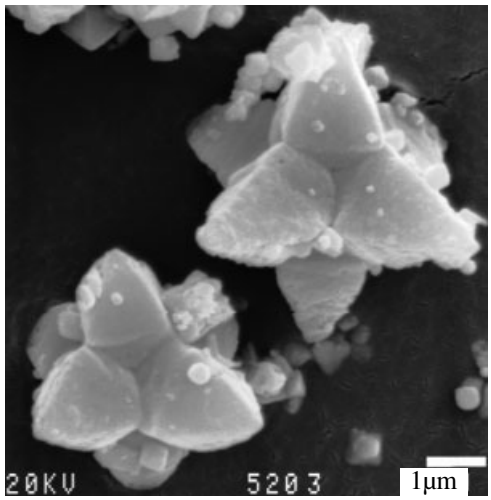

Figure 10. Scanning-electron micrograph of a cuprous oxide powder. Reactor 5^c. Experiment 2. Electrolyte: 250 g dm^{-3} NaCl, 5 g dm^{-3} calcium gluconate, pH = 10, $T = 80^{\circ}C$. Magnification: ×10000.

that the separator complements the inhibiting effect of calcium gluconate on the cuprous oxide reduction and metallic copper was not detected in the powder. However, these experiments reveal as a drawback a low value of anodic current efficiency at the bipolar electrode because of the leakage current. The last rows of Table 4 show the composition of powders obtained in experiments with plastic protectors at the upper and lower ends of the bipolar electrode, reactor 5^c. Likewise, Fig. 9 reports that the cuprous oxide concentration increases when the current is increased, with the exception of the value obtained at the highest current. Thus, the oxidation of copper to cuprous oxide is also kinetically favoured over cupric oxide production, which was scarcely detected in the powders obtained at current densities ranging from 21 to 103 mA cm^{-2}, currents from 4.2 A to 10 A in reactor 5^c, in spite of its formation is thermodynamically possible. It must be recognized that Vetere and Romagnoli[9] have proposed higher anodic current densities (up to 200 mA cm^{-2}), using sodium nitrate in the electrolyte. Under this condition, hydroxylamine is produced at the cathode, which probably reduces the cupric oxide formed at higher anodic current densities. Under the conditions examined, a red colour for cuprous oxide powder was obtained.

Figure 10 shows the morphology of cuprous oxide powder with an octahedral shape, which agrees with a previous study[12] with a smooth surface electrode. The size of the particles is very small, approximately 2 microns.

CONCLUSIONS

1 Two beneficial aspects can be recognized in calcium gluconate as an additive for the electrochemical production of cuprous oxide: (i) to decrease the cell voltage due to the depolarization of hydrogen evolution; and (ii) to avoid the reduction of cuprous oxide to metallic copper at very negative potentials where hydrogen evolution takes place.
2 Special care should be taken in the design aspects of the electrochemical reactor to minimize the leakage current, which is the main drawback of the bipolar connection.
3 Three-dimensional anodes allow the production of cuprous oxide from scrap copper. However, copper particles were detected in the powders as a consequence of the mechanical deterioration of the anode, which can be separated by fractioned sedimentation to improve the quality of the powders.
4 Bipolar electrochemical reactors represent suitable devices for the production of cuprous oxide owing to their simplified construction features showing a similar quality in the product with respect to the monopolar arrangements.

ACKNOWLEDGEMENTS

This work was supported by the Agencia Nacional de Promoción Científica y Tecnológica (ANPCyT), Consejo Nacional de Investigaciones Científicas y Técnicas (CONICET) and Universidad Nacional del Litoral (UNL) of Argentina.

REFERENCES

1 Pletcher D and Walsh FC, *Industrial Electrochemistry*. Chapman and Hall, London, 290 (1993).
2 Lossin A and Westhoff FJ, The production and application of cuprous oxide and cupric hydroxide. *JOM* October: 38–39 (1997).
3 Kirk RE and Othmer DF, *Encyclopedia of Chemical Technology*, Volume **7**, 4th edn. Wiley-Interscience, New York, 254 (1993).
4 Musa AO, Akomolafe T and Carter MJ, Production of cuprous oxide, a solar cell material, by thermal oxidation and a study of its physical and electrical properties. *Sol Energy Mater Sol Cells* **51**:305–316 (1998).
5 Dong Y, Li Y, Wang C, Cui A and Deng Z, Preparation of cuprous oxide particles of different crystallinity. *J Colloid Interface Sci* **243**:85–89 (2001).
6 Muramatsu A and Sugimoto T, Synthesis of uniform spherical Cu_2O particles from condensed CuO suspensions. *J Colloid Interface Sci* **189**:167–173 (1997).
7 Konishi Y, Nomura T and Satoh D, Solvothermal preparation of cuprous oxide fine particles by hydrolysis of copper (II) carboxylate in two-phase liquid-liquid system. *Ind Eng Chem Res* **43**:2088–2092 (2004).
8 Vetere V, Romagnoli R and Carbonari RO, Aplicación de las curvas de polarización al estudio del proceso electroquímico de obtención de óxido cuproso. *CIDEPINT-An* 31–42 (1983). (In Spanish).
9 Vetere VF and Romagnoli R, Processes of elaboration of cuprous oxide. Study of variables in the chemical reduction of cupric sulfate and electrochemical oxidation of metallic copper. *Ind Eng Chem Prod Res Dev* **23**:656–658 (1984).
10 Vetere VF and Romagnoli R, Application of polarization curves to the study of the electrochemical process for producing cuprous oxide. *J Chem Technol Biotechnol* **34**:335–340 (1984).
11 Ji J and Cooper WC, Electrochemical preparation of cuprous oxide powder: Part I. Basic electrochemistry. *J Appl Electrochem* **20**:818–825 (1990).
12 Ji J and Cooper WC, Electrochemical preparation of cuprous oxide powder: Part II. Process conditions. *J Appl Electrochem* **20**:826–834 (1990).
13 Palanisamy R, Narasimham KC, Viswanathan R and Udupa HVK, Electrolytic production of cuprous oxide. *Indian J Technol* **22**:319–320 (1984).
14 Figueroa MG, Gana RE, Cooper WC and Ji J, Electrochemical production of cuprous oxide using the anode-support system. *J Appl Electrochem* **23**:308–315 (1993).
15 Gana R, Figueroa M, Aragón A, San Martín MT and Kattan L, Electrochemical production of cuprous oxide and metallic nickel in a two-compartment cell. *J Appl Electrochem* **24**:542–547 (1994).
16 Pletcher D and Walsh FC, *Industrial Electrochemistry*. Chapman and Hall, London, 136 (1993).
17 Qingxue Z, Effect of additives on electrolytic manufacture of cuprous oxide. *Chinese J Nonferrous Metals* **10**:127–130 (2000).

